● RESEARCH ARTICLE

Microstructural damage pattern of vascular cognitive impairment: a comparison between moyamoya disease and cerebrovascular atherosclerotic disease

Jia-Bin Su[1, #], Si-Da Xi[2, #], Shu-Yi Zhou[3], Xin Zhang[1], Shen-Hong Jiang[1], Bin Xu[1], Liang Chen[1], Yu Lei[1, *], Chao Gao[1, *], Yu-Xiang Gu[1]
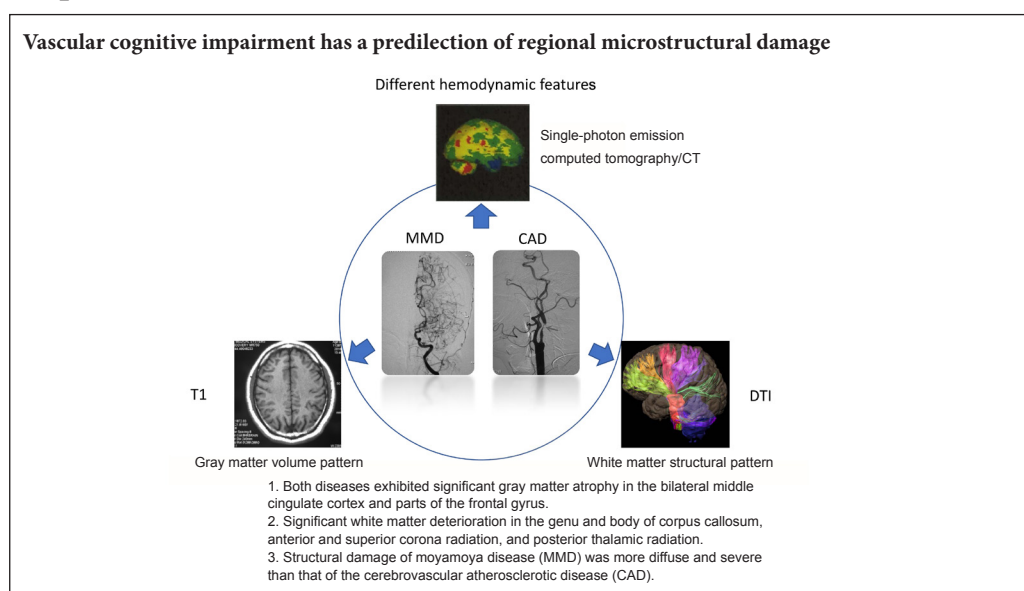
1 Department of Neurosurgery, Huashan Hospital, Fudan University, Shanghai, China
2 Shanghai Medical College, Fudan University, Shanghai, China
3 Department of Radiology, Huashan Hospital, Fudan University, Shanghai, China

Graphical Abstract

Vascular cognitive impairment has a predilection of regional microstructural damage

1. Both diseases exhibited significant gray matter atrophy in the bilateral middle cingulate cortex and parts of the frontal gyrus.
2. Significant white matter deterioration in the genu and body of corpus callosum, anterior and superior corona radiation, and posterior thalamic radiation.
3. Structural damage of moyamoya disease (MMD) was more diffuse and severe than that of the cerebrovascular atherosclerotic disease (CAD).

Correspondence to:
Chao Gao, MD,
thunderstormer@126.com;
Yu Lei, MD,
piliyouxia_lei@126.com.

#These authors contributed equally to this paper.

orcid:
0000-0003-2245-0582
(Jia-Bin Su)

Abstract

Moyamoya disease and cerebrovascular atherosclerotic disease are both chronic ischemic diseases with similar presentations of vascular cognitive impairment. The aim of the present study was to investigate the patterns of microstructural damage associated with vascular cognitive impairment in the two diseases. The study recruited 34 patients with moyamoya disease (age 43.9 ± 9.2 years; 20 men and 14 women, 27 patients with cerebrovascular atherosclerotic disease (age: 44.6 ± 7.6 years; 17 men and 10 women), and 31 normal controls (age 43.6 ± 7.3 years; 18 men and 13 women) from Huashan Hospital of Fudan University in China. Cognitive function was assessed using the Mini-Mental State Examination, long-term delayed recall of Auditory Verbal Learning Test, Trail Making Test Part B, and the Symbol Digit Modalities Test. Single-photon emission-computed tomography was used to examine cerebral perfusion. Voxel-based morphometry and tract-based spatial statistics were performed to identify regions of gray matter atrophy and white matter deterioration in patients and normal controls. The results demonstrated that the severity of cognitive impairment was similar between the two diseases in all tested domains. Patients with moyamoya disease and those with cerebrovascular atherosclerotic disease suffered from disturbed supratentorial hemodynamics. Gray matter atrophy in bilateral middle cingulate cortex and parts of the frontal gyrus was prominent in both diseases, but in general, was more severe and more diffuse in those with moyamoya disease. White matter deterioration was significant for both diseases in the genu and body of corpus callosum, in the anterior and superior corona radiation, and in the posterior thalamic radiation, but in moyamoya disease, it was more diffuse and more severe. Vascular cognitive impairment was associated with regional microstructural damage, with a potential link between, gray and white matter damage. Overall, these results provide insight into the pathophysiological nature of vascular cognitive impairment. This study was approved by the Institutional Review Board in Huashan Hospital, China (approval No. 2014-278). This study was registered with ClinicalTrials.gov on December 2, 2014 with the identifier NCT02305407.

Chinese Library Classification No. R445; R741

Introduction

Vascular cognitive impairment represents the entire spectrum of cognitive impairments associated with vascular pathology, ranging from mild cognitive impairment to fully developed dementia (Gorelick et al., 2011; Zhao et al., 2012a). Deficits in executive function/attention are regarded as hallmarks of vascular cognitive impairment and have been related to chronic deficiencies in frontal blood flow (O'Brien et al., 2003; Hachinski et al., 2006). In our previous studies, we characterized the neuropsychological, hemodynamic, and structural changes of early stage vascular cognitive impairment (Cao et al., 2010; Lei et al., 2016). However, the details regarding microstructural damage in vascular cognitive impairment remain unclear.

Moyamoya disease and cerebrovascular atherosclerotic disease are both chronic progressive cerebrovascular steno-occlusive diseases that are commonly reported in the field of vascular cognitive impairment with prolonged cerebral hypoperfusion (Weinberg et al., 2011; Marshall et al., 2014). In cases of both adult moyamoya disease and adult cerebrovascular atherosclerotic disease, vascular cognitive impairment has been documented as the consequence of ischemic damage that resulted from dynamic factors such as cerebral hypoperfusion rather than to abnormal brain structure (Bos et al., 2012; Karzmark et al., 2012). Thus, studies of moyamoya disease and cerebrovascular atherosclerotic disease offer us a good chance to understand the characteristics of vascular cognitive impairment.

Although the two diseases share similar clinical vascular cognitive impairment features, the etiology and pathogenesis of their vascular cognitive impairments are apparently different. Vascular cognitive impairment in moyamoya disease is associated with an inflammatory process of the central nervous system and is characterized by the development of collateral vessels that compensate for the significant narrowing of the basal vasculature (Soriano et al., 2002; Kazumata et al., 2015). In contrast, vascular cognitive impairment in cerebrovascular atherosclerotic disease is associated with both calcified atherosclerotic plaque lesions and arterial intima-media thickness, irrespective of demographic characteristics or major vascular risk factors (van Oijen et al., 2007; Bos et al., 2012; Wendell et al., 2012; Reis et al., 2013). Additionally, compared with cerebrovascular atherosclerotic disease, cerebral blood flow in moyamoya disease is reported to be both relatively centrally preserved and consistently high in all supratentorial regions (Obara et al., 1997; Schubert et al., 2014).

Focal atrophy of the cerebral cortex is reported to be caused by chronic regional hemodynamic disturbances and contribute to the development of vascular cognitive impairment (Wendell et al., 2012; Lei et al., 2016). Additionally, cerebral white matter is highly vulnerable to ischemia (Pantoni et al., 1996; Vermeer et al., 2003), and the Wallerian degeneration of axons projecting from cortical regions related to cognitive performance is another proposed mechanism underlying vascular cognitive impairment (Balucani and Silvestrini, 2011; Calviere et al., 2012). To the best of our knowledge, few reports have evaluated these two major diseases that include vascular cognitive impairment, particularly in terms of their respective microstructural damage. Based on a recent study that compared perfusion patterns in moyamoya disease and cerebrovascular atherosclerotic disease (Schubert et al., 2014), we hypothesize that the spatial patterns of microstructural damage in these two diseases are similar to their perfusion patterns. The aim of the present study was to investigate the pattern of microstructural damage in vascular cognitive impairment by comparing the two diseases, thus helping us better understand the pathophysiology of vascular cognitive impairment.

Participants and Methods

Participants

Thirty-four adult patients with moyamoya disease and twenty-seven patients with cerebrovascular atherosclerotic disease were consecutively enrolled at the department of neurosurgery between May and August 2013 and matched for demographic characteristics. Patients were diagnosed based on digital subtraction angiography and in accordance with published guidelines (Research Committee on the Pathology and Treatment of Spontaneous Occlusion of the Circle of Willis and Health Labour Sciences Research Grant for Research on Measures for Infractable Diseases, 2012). All participants were Chinese nationals aged 18–60 years, right-handed, with no evidence of infarct in the cerebral cortex, basal ganglia, brainstem, cerebellum, or any intracerebral hemorrhage. Participants with cysts in their cerebral subcortical white or with small spots of hyperintense signals smaller than an arbitrary cutoff of 8 mm on T2 images were included (Hachinski et al., 2006; Lei et al., 2016). Patients with extracranial internal carotid artery stenosis or occlusion were excluded from the cerebrovascular atherosclerotic disease group, and patients with only unilateral vascular damage were ruled out from both groups to keep them more comparable. Through advertisements, we also recruited 31 normal controls with matching demographic features from the Shanghai community in China. Control participants were without cerebrovascular disease, as determined by magnetic resonance angiography. All patients received standard anti-platelets before being enrolled in the study. Participants were excluded if they exhibited significant neurological or psychiatric disorders, had severe systemic diseases, or presented with uncontrolled vascular risk factors that could affect cognition, such as hypertension, diabetes, dyslipidemia, drug abuse, or alcoholism. National Institutes of Health Stroke Scale (NIHSS) scores of all patients were assessed by two qualified neurosurgeons.

This study was approved by the Institutional Review Board in Huashan Hospital, China (approval No. 2014-278) (**Additional file 1**) and was conducted in accordance with the *Declaration of Helsinki*. All participants or their legal guardians provided informed consent. The trial was registered with Clinicaltrials.gov on December 2, 2014 (identifier NCT02304507) and the protocol version number is 1.0. A flowchart of the study is shown in **Figure 1**. This study follows the STrengthening the Reporting of OBservational studies in Epidemiology (STROBE) guidance (**Additional file 2**).
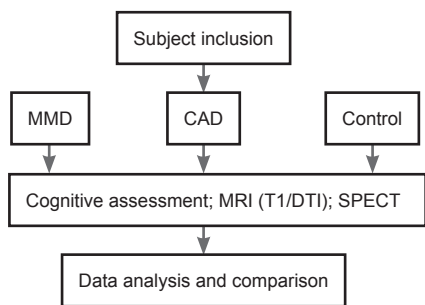
Figure 1 Flow chart for the study.
MMD: Moyamoya disease; CAD: cerebrovascular atherosclerotic disease; SPECT: single-photo emission computed tomography.

Neuropsychological assessment

An eligible neuropsychologist who was blinded to the patient diagnoses administered the neuropsychological tests. Global cognitive state was evaluated with the Mini-Mental State Examination (Chua et al., 2018). Additionally, long-term delayed recall results from long-term delayed recall of the Auditory Verbal Learning Test was used to assess episodic memory (Zhao et al., 2012b). The Trail Making Test Part B and the Symbol Digit Modalities Test were used to assess attention/executive function (Lu and Bigler, 2002; Wei et al., 2018). Specific cognitive assessment methods have been explained in detail in previous studies (Lei et al., 2014, 2016, 2017a, b).

Magnetic resonance imaging (MRI)

An experienced technician, unaware of the study's purpose, performed the MRI scans. All MRI scans were performed on a 3.0 Tesla scanner (GE Healthcare, GE Asian Hub, Shanghai, China) using a 32-channel intraoperative head coil. The diffusion-weighted images were acquired using a single-shot spin-echo planar imaging sequence with the following parameters: 43 interleaved contiguous axial slices, slice thickness = 1.5 mm, repetition time = 8600 ms, flip angle = 90°, field of view = 270×270 mm^2, matrix size = 128×128, number of excitations = 1, 30 diffusion-weighted volumes with non-collinear directions ($b = 1000$ s/mm^2), and five non-diffusion-weighted volumes ($b = 0$ s/mm^2). Total acquisition time was approximately 15 minutes.

Image preprocessing

Patterns of gray matter atrophy

To investigate differences in gray matter atrophy among the three groups, voxel-based morphometry (VBM) was carried out on all structural images using the VBM8 tool kit (http://dbm.neuro.uni-jena.de) for Statistical Parametric Mapping (SPM8, http://www.fil.ion.ucl.ac.uk/spm/) in the MATLAB environment (The MathWorks Inc., Natick, Massachusetts, United States). Preprocessing steps included: (1) normalizing the anatomical images using a high-dimensional nonlinear diffeomorphic registration algorithm by DARTEL to the Montreal Neurological Institute (MNI) template in 1.5 mm cubic resolution; (2) segmenting the spatially normalized images into gray matter, white matter, and cerebrospinal fluid; (3) smoothing the images with an 8-mm Gaussian kernel; (4) calculating the whole-brain gray matter volume for each group.

Patterns of white matter deterioration

Diffusion-tensor imaging (DTI) data were examined for artifacts and signal dropout before pre-processing using the FMRIB Software Library view. High-quality DTI data were corrected according to the following criteria. FMRIB Software Library version 5.0 (http://www.fmrib.ox.ac.uk/fsl) was used for pre-processing. First, each participant's original data were corrected for eddy-current distortions and head motions using the eddy-correct command in FMRIB's Diffusion Toolbox. The correction was carried out by registering the individual volumes to the b0 images. Next, the skull was removed from the b0 image using the Brain Extraction Tool (http://fsl.fmrib.ox.ac.uk/fsl/fslwiki/BET) (Smith, 2002) and the corresponding brain mask was applied to the eddy-corrected diffusion-weighted images. Fractional anisotropy (FA) and mean diffusivity (MD) of each voxel were calculated using the 'dtifit' command in FMRIB's Diffusion Toolbox.

Tract-based spatial statistics were applied to the FA and MD values using FMRIB's Diffusion Toolbox to investigate white matter integrity and diffusion characteristics. Individual FA images were registered non-linearly to the FMRIB58 template in MNI space and then averaged over all individuals to generate a mean FA image. Next, a study-specific FA skeleton was created from the generated mean FA map, which represented the core of the white matter tracts for all participants. The FA values were thresholded at 0.2 to avoid including any gray matter. Each subject's FA and MD images were projected onto this skeleton. The between-group difference was examined using FMRIB Software Library's permutation tool (1000 permutations) with the inclusion of gender and age as covariates, and a cluster significance level of $P < 0.05$, corrected with threshold-free cluster enhancement.

Evaluation of hemodynamic status

Single-photon emission-computed tomography/CT (Siemens, Symbia T16, Erlangen, Germany) was used to evaluate perfusion values in each brain region. Patients relaxed in the Oblique position, closing their eyes in a dark and quiet room for 30 minutes, and single-photon emission-computed tomography/CT scans were obtained after an intravenous injecting 1480 MBq of ^{99m}Tc-ethyl cysteinate dimer (Neurolite, Bristol-Myers Squibb Pharma). Data were collected into a 128×128 matrix through a 360° rotation at steps of 2.8° for 80,000 counts per view. Filtered back-projection was employed using ordered subset-expectation materialization for reconstructing the images. Quantification of ach brain-perfusion single-photon emission-computed tomography/CT study was accomplished using the NeuroGam software package (Segami Corporation). This software applies AFNI anatomical coregistration through blocks of data defined in the Talairach space. The acquisition time for single-photon emission computed tomography/CT was 30 minutes

Specific tracer-uptake ratios were bilaterally assessed for the region of interests in four consecutive transverse slices with highest radioactivity, and the arithmetic mean of these four slices was calculated. The cerebellums served as the reference regions and were drawn in the same way on two consecutive

transverse slices. The specific tracer-uptake ratio was calculated as target divided by cerebellum, where the target represented bilateral frontal lobe, parietal lobe, occipital lobe, or thalamus.

Statistical analysis

Statistical analysis and database management were performed using SPSS 17.0 software (SPSS Inc., Chicago, IL, USA). Differences among groups were tested *via* one-way analysis of variance, Fisher's exact test, and Kruskal-Wallis rank test, while *post hoc* tests with Bonferroni correction were used for further comparisons. Significance was set at $P < 0.05$.

Voxel-wise comparison was carried out on gray matter volumes using SPM8. Results were assessed at $P < 0.05/3$ (FDR corrected) for multiple comparisons. Skeletonized FA and MD maps were analyzed *via* group comparison. Voxel-wise statistics was performed across participants using Randomise, a FMRIB Software Library tool for nonparametric permutation. A null distribution was built for each contrast based on 5000 random permutations. Threshold-free cluster enhancement with corrected $P < 0.05/3$ was used in the comparison (Hua et al., 2008). For visualization purposes, tracts were dilated using the "tbss-fill" command from the FMRIB Software Library. Regions in major white matter tracts that exhibited significant changes in FA and MD were later defined using the John Hopkins University white matter atlases in MNI space (Wakana et al., 2007; Avelar et al., 2015).

Results

Demographic, neuropsychological, and hemodynamic features for patients with moyamoya disease or cerebrovascular atherosclerotic disease and for normal controls

Patient characteristics are summarized in **Table 1**. The three groups did not show significant differences in age, sex, education level, or controlled vascular risk factors, except for treated for hypercholesterolemia ($F = 1.222$; $P < 0.05$). Further, National Institutes of Health Stroke Scale (NIHSS) scores did not differ between the two patient groups (moyamoya disease *vs.* cerebrovascular atherosclerotic disease: 1.5 ± 1.8 *vs.* 1.8 ± 1.7; $z = 0.676$, $P = 0.499$).

Significant group differences were found for Mini-Mental State Examination ($F = 14.738$; $P = 0.006$), long-term delayed recall of Auditory Verbal Learning Test ($F = 9.96$; $P < 0.001$), Symbol Digit Modalities Test ($F = 16.447$; $P < 0.001$), and The Trail Making Test Part B scores ($F = 24.138$; $P < 0.001$). Further analysis indicated that patients with moyamoya disease performed significantly worse than normal controls on the Mini-Mental State Examination ($z = 3.375$, $P < 0.001$), long-term delayed recall of Auditory Verbal Learning Test ($P < 0.001$), Symbol Digit Modalities Test ($z = 4.555$, $P < 0.001$), and The Trail Making Test Part B ($z = 3.953$, $P < 0.001$). Similarly, patients with cerebrovascular atherosclerotic disease performed significantly worse than normal controls on the Mini-Mental State Examination ($z = 3.307$, $P < 0.001$), long-term delayed recall of Auditory Verbal Learning Test ($P = 0.015$), Symbol Digit Modalities Test ($z = 3.613$, $P < 0.001$), and The Trail Making Test Part B ($z = 2.801$, $P = 0.005$). However, no significant differences were found between the two patient groups on any of these neuropsychological tests. Both moyamoya disease and cerebrovascular atherosclerotic disease group demonstrated lower perfusion in supratentorial regions compared with the control group. *Post hoc* analysis showed lower perfusion in the thalamus of the cerebrovascular atherosclerotic disease group than in the control group, but the difference was not significant. The hemodynamic features among the three groups showed a moyamoya disease < cerebrovascular atherosclerotic disease < controls pattern for all brain regions except the left occipital lobe (**Table 2**).

Gray matter atrophy patterns among moyamoya disease patients, cerebrovascular atherosclerotic disease patients, and normal controls

Differences in gray matter volume among the three groups are highlighted in **Figure 2** (corrected $P < 0.05/3$). Compared

Table 1 Demographic and neuropsychological features for patients and normal controls

Index	MMD ($n = 34$)	CAD ($n = 27$)	Normal controls ($n = 31$)	F/χ^2 value (P value)
Age (years)	43.9±9.2	44.6±7.6	43.6±7.3	0.528(0.768)
Men	20(58.8)	17(63.0)	18(58.1)	0.165(0.921)
Education (years)	8.7±5.1	9.7±3.9	9.4±4.0	0.933(0.627)
Treated hypertension	11(32.4)	12(44.4)	10(32.3)	1.222(0.543)
Treated hypercholesterolemia	10(29.4)	23(85.2)	7(22.6)	(< 0.001)[a]
Treated diabetes	5(14.7)	7(25.9)	3(9.7)	(0.257)[a]
Smoking	12(35.3)	11(40.7)	9(29.0)	0.878(0.645)
Cognitive status				
MMSE	25.3±3.8	26.4±2.1	28.2±1.7	14.738(0.006)[b]
AVLT-LR	3.2±2.6	4.1±2.8	6.2±2.8	9.96(< 0.001)
TMT-B (seconds)	178.2±58.3	161.6±60.0	119.0±37.3	16.447(< 0.001)[b]
SDMT	26.8±14.3	32.4±13.7	43.1±9.3	24.138(< 0.001)[b]

Data are expressed as the mean ± SD for age, education, and cognitive status assessment results, and number (percent) in other indices, [a]Fisher's exact test. [b]Kruskal-Wallis rank test. MMSE: Mini-Mental State Examination; AVLT-LR: long-term delayed recall of the Auditory Verbal Learning Test (a 20-minute delay time); TMT: Trail Making Test; TMT-B: time of TMT Part B; SDMT: Symbol Digit Modalities Test; MMD: moyamoya disease; CAD: cerebrovascular atherosclerotic disease.

with controls, the moyamoya disease group exhibited widespread loss of gray matter volume, particularly in the frontal cortex (bilateral middle frontal gyrus, middle cingulate cortex, left superior frontal gyrus, and left orbitofrontal gyrus). Compared with controls, the cerebrovascular atherosclerotic disease group exhibited significantly lower gray matter volume in the frontal cortex (particularly in left medial superior frontal gyrus and bilateral middle cingulate cortex) and the parietal cortex (left superior parietal gyrus). Interestingly,

the cerebrovascular atherosclerotic disease group presented a pattern of gray matter atrophy in the medial part of the brain.

Gray matter volume was significantly less in the moyamoya disease group than in the cerebrovascular atherosclerotic disease group for the left superior frontal gyrus, left middle frontal gyrus, and left precuneus. In contrast, gray matter volume was significantly less in the cerebrovascular atherosclerotic disease group than in the moyamoya disease group for the left medial superior frontal gyrus and bilateral

Table 2 Hemodynamic differences among patients and normal controls
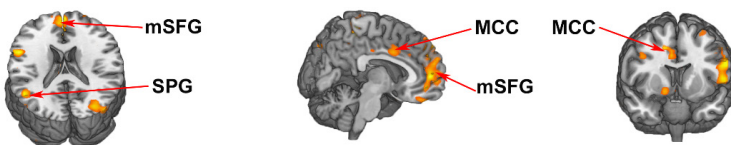
	MMD	CAD	Normal controls	P value	Normal controls vs. MMD patients	Normal controls vs. CAD patients	MMD patients vs. CAD patients
					Adjusted P value		
Left frontal cortex	0.82±0.03	0.86±009	0.98±0.06	0.003	0.001	0.009	0.335
Right frontal cortex	0.84±0.13	0.87±0.11	0.98±0.09	0.001	< 0.001	0.004	0.09
Left parietal cortex	0.91±0.13	0.92±0.10	1.05±0.08	0.001	0.001	0.001	0.941
Right parietal cortex	0.87±0.13	0.93±0.11	1.05±0.11	0.001	< 0.001	0.012	0.136
Left temporal cortex	0.83±0.11	0.84±0.09	0.93±0.06	0.006	0.002	0.008	0.597
Right temporal cortex	0.83±0.11	0.87±0.10	0.96±0.08	0.007	0.002	0.029	0.232
Left occipital cortex	1.07±0.15	1.07±0.10	1.13±0.09	0.262	0.11	0.187	0.765
Right occipital cortex	0.84±0.13	0.87±0.11	0.98±0.09	0.02	0.15	0.247	0.063
Left thalamus	0.80±0.15	0.87±0.10	0.96±0.08	0.03	0.03	0.683	0.028
Right thalamus	0.79±0.14	0.91±0.06	0.93±0.11	< 0.001	< 0.001	0.644	<0.001

Data are expressed as the tracer uptake radio (mean ± SD; one-way analysis of variance followed by Bonferroni *post hoc* test). MMD: Moyamoya disease; CAD: cerebrovascular atherosclerotic disease.
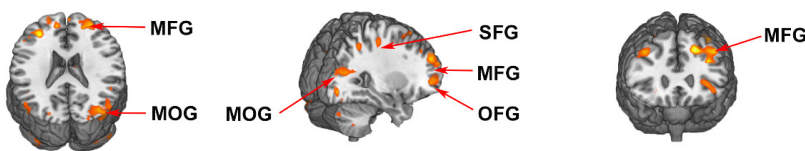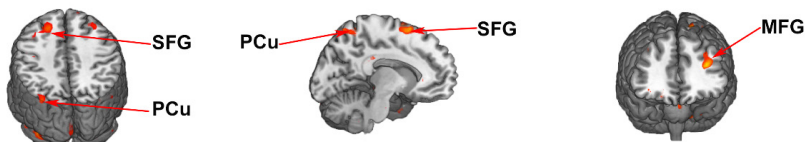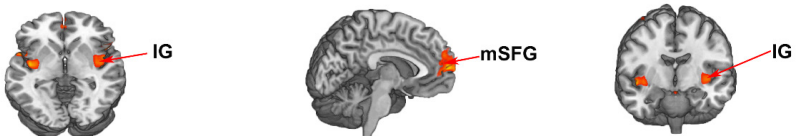
Figure 2 Comparison of gray matter volume (MRI T1) among patients and normal controls.
(A) Gray matter volume (GMV) reduction in MMD compared with controls; (B) GMV reduction in CAD compared with NC; (C) GMV reduction in MMD compared with CAD; (D) GMV reduction in CAD compared with MMD. Significance threshold set at FDR-corrected *P* < 0.05/3. Colored bars represent Z values. GMV: Gray matter volume; MMD: moyamoya disease; CAD: cerebrovascular atherosclerotic disease; NC: normal controls; MFG: middle frontal gyrus; MOG: middle occipital gyrus; SFG: superior frontal gyrus; OFG: orbitofrontal gyrus; mSFG: medial superior frontal gyrus; SPG: superior parietal gyrus; MCC: middle cingulate cortex; PCu: precuneus; IG: insular gyrus.

insular gyrus (**Table 3**).

White matter deterioration patterns among moyamoya disease patients, cerebrovascular atherosclerotic disease patients, and normal controls

We further looked for white matter deterioration patterns in the two patient groups (**Figure 3**; corrected $P < 0.05/3$; threshold-free cluster enhancement). Compared with controls, FA was significantly lower and MD was significantly higher throughout widespread white matter tracts in the moyamoya disease group. Lower FA was observed in the genu, body, and splenium of the corpus callosum, the in-

Table 3 Z-statistical maps of gray matter volume differences among patients and normal controls

	Brain regions	Volume (mm³)	MNI coordinates (mm)			Maximum Z
			x	y	z	
NC *vs.* MMD	Right middle frontal gyrus	3834	30	51	33	5.937
	Left middle frontal gyrus	7614	−30	45	27	5.767
	Left middle cingulate cortex	1728	−9	−3	39	5.204
	Right middle cingulate cortex	1476	9	0	36	5.126
	Left superior frontal gyrus	4482	−21	−6	60	4.854
	Left orbitofrontal gyrus	1746	−18	60	−12	4.478
	Left middle occipital gyrus	1332	−24	−72	30	4.465
	Right middle occipital gyrus	2205	36	−78	27	4.140
	Right middle temporal gyrus	1935	48	−27	−6	4.074
NC *vs.* CAD	Left medial superior frontal gyrus	7911	−9	60	12	5.333
	Left superior parietal gyrus	1539	−18	−69	45	5.074
	Right middle cingulate cortex	2592	12	6	42	4.885
	Left middle cingulate cortex	2061	−3	−42	54	3.801
CAD *vs.* MMD	Left superior frontal gyrus	1512	−18	9	60	4.451
	Left middle frontal gyrus	1323	−33	39	21	4.340
	Left precuneus	792	−9	−66	57	3.606
MMD *vs.* CAD	Left medial superior frontal gyrus	2025	−3	60	9	3.937
	Right insular gyrus	1242	45	0	−6	3.598
	Left insular gyrus	729	−42	−6	−3	3.525

x, y, z: Peak MNI coordinates; *Z*: statistical value for the voxel showing peak gray matter volume differences among groups (adjusted for age and sex, corrected *P* < 0.05/3). MNI: Montreal Neurological Institute; NC: normal control; MMD: moyamoya disease; CAD: cerebrovascular atherosclerotic disease.
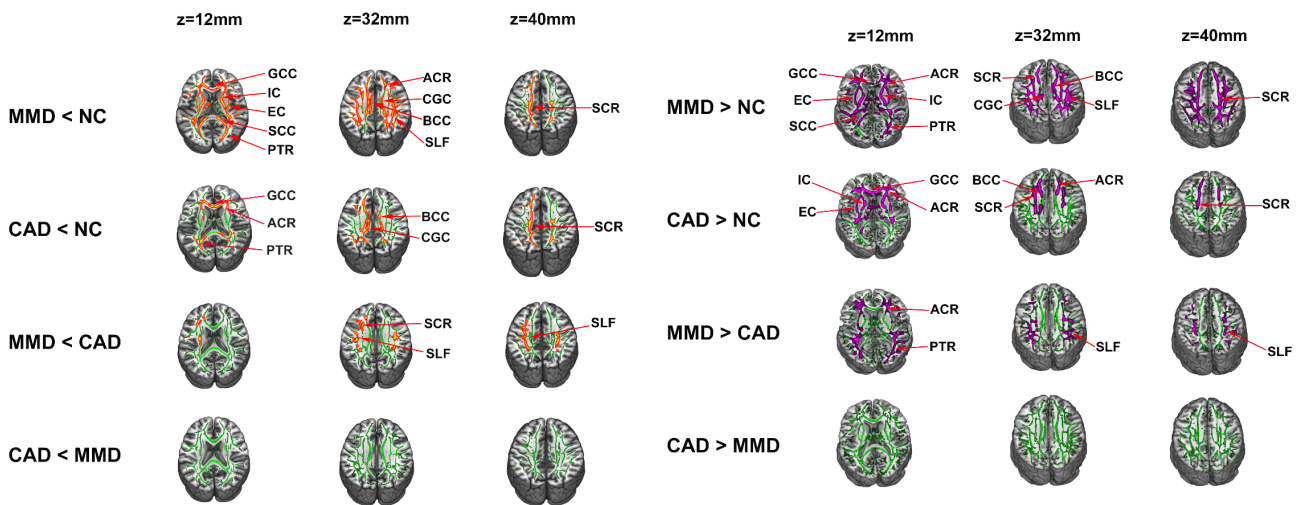
Figure 3 Tract-based spatial statistical analysis (Montreal Neurological Institute diffusion-tensor imaging) of FA decrease and MD increase among patients and normal controls.
(A) FA decrease (red); (B) MD increase (purple). Demographic variables were controlled for and results are overlaid on the MNI152 template and the mean diffusion tensor imaging metrics skeleton (green). Significance: corrected *P* < 0.05/3; threshold-free cluster enhancement. ACR: Anterior corona radiate; BCC: body of corpus callosum; SCC: splenium of the corpus callosum; PTR: posterior thalamic radiation; CGC: cingulum; EC: external capsule; GCC: genu of corpus callosum; IC: internal capsule; SLF: superior longitudinal fasciculus; SCR: superior corona radiate; NC: normal controls; FA: Fractional anisotropy; MD: mean diffusivity; MMD: moyamoya disease; CAD: cerebrovascular atherosclerotic disease.

ternal and external capsule, anterior and superior corona radiation, cingulum, superior longitudinal fasciculus, and a portion of the posterior thalamic radiation. Higher MD was more extensive in the same white matter tracts. No regions of significantly higher FA or significantly lower MD were found in the moyamoya disease group.

Similarly, we found that FA was significantly lower and MD was significantly higher in the central part of the white matter tracts in the cerebrovascular atherosclerotic disease group compared with controls, including a portion of the genu and body of corpus callosum, cingulum, posterior thalamic radiation, anterior corona radiata, and part of superior corona radiata. Higher MD was more extensive in these same white matter tracts. In addition, higher MD was also found in the bilateral internal and external capsule of the cerebrovascular atherosclerotic disease group. FA was not higher in the cerebrovascular atherosclerotic disease group than in controls, nor was MD lower (**Tables 4** and **5**).

The white matter damage was more diffuse and severe in the moyamoya disease group than in the cerebrovascular atherosclerotic disease group. In particular, FA was significantly lower in the moyamoya disease group in parts of the anterior and superior corona radiata and in the superior longitudinal fasciculus. Moreover, higher MD was primarily found in part of the anterior corona radiata, posterior thalamic radiation, and superior longitudinal fasciculus. In contrast, the cerebrovascular atherosclerotic disease group did not exhibit any significantly lower FA or any significantly higher MD than the moyamoya disease group (**Tables 4** and **5**).

Discussion

To date, with increasing reports of cognitive impairment in patients with chronic cerebrovascular diseases, the diagnoses and treatments of vascular cognitive impairment are becoming more of a concern (Gorelick et al., 2011; Kazumata et al., 2015; Meng et al., 2017; He et al., 2018; Weinstein, 2018). However, most published studies of vascular cognitive impairment are based on only a single disease, making it difficult to discern common vascular cognitive impairment features from individual disease pathophysiology. In the present study, we conducted a cross-sectional neuroimaging analysis of two chronic cerebrovascular diseases commonly reported in the field of vascular cognitive impairment. Results indicated that (1) moyamoya disease and cerebrovascular atherosclerotic disease exhibited supratentorial impaired cerebral perfusion, with greater hypoperfusion in the moyamoya disease group; (2) moyamoya disease and cerebrovascular atherosclerotic disease groups exhibited significant gray matter atrophy in the bilateral middle cingulate cortex and parts of the frontal gyrus, with but the atrophy in the moyamoya disease group being more diffuse and severe; (3) moyamoya disease and cerebrovascular atherosclerotic disease groups showed significant white matter deterioration in the genu and body of corpus callosum, anterior and superior corona radiations, cingulum, and posterior thalamic radiation. White matter deterioration in the moyamoya disease group was more diffuse and severe than that in the cerebrovascular atherosclerotic disease group.

Previous studies have reported structural and functional

Table 4 Permutation test for differences in fractional anisotropy among patients and normal controls

| | Cluster | Volume (mm³) | MNI coordinates (mm) | | | P | Anatomical region |
			x	y	z		
NC *vs.* MMD	1	7529	42	–6	–16	< 0.05/3	Genu of corpus callosum
							Internal capsule
							External capsule
							Splenium of the corpus callosum
							Posterior thalamic radiation
	2	786	–30	–60	–4	< 0.05/3	Anterior corona radiate
							Cingulum
							Body of corpus callosum
							Superior longitudinal fasciculus
	3	279	26	–58	38	< 0.05/3	Left superior corona radiate
NC *vs.* CAD	1	3041	8	–26	4	< 0.05/3	Genu of corpus callosum
							Left anterior corona radiate
							Right posterior thalamic radiation
	2	789	14	48	26	< 0.05/3	Body of corpus callosum
							Cingulum
	3	247	–24	–44	46	< 0.05/3	Left superior corona radiate
CAD *vs.* MMD	1	237	–32	–20	54	< 0.05/3	Left superior corona radiate
							Left superior longitudinal fasciculus

Results are bilateral unless a hemisphere is specified. *x, y, z*: Peak coordinates in MNI space. MNI: Montreal Neurological Institute; MMD: moyamoya disease; CAD: cerebrovascular atherosclerotic disease; NC: normal control.

Table 5 Permutation test for differences in mean diffusivity among patients and normal controls

	Cluster	Volume (mm³)	MNI coordinates (mm)			P	Anatomical region
			x	y	z		
NC *vs.* MMD	1	6431	43	−10	−15	< 0.05/3	Genu of corpus callosum
							Internal capsule
							External capsule
							Splenium of the corpus callosum
							Anterior corona radiate
							Posterior thalamic radiation
	2	783	−29	−63	−5	< 0.05/3	Superior corona radiate
							Cingulum
							Body of corpus callosum
							Superior longitudinal fasciculus
	3	280	27	−60	42	< 0.05/3	Superior corona radiate
NC *vs.* CAD	1	3022	9	−39	5	< 0.05/3	Genu of corpus callosum
							Anterior corona radiate
							External capsule
							Internal capsule
	2	801	16	50	29	< 0.05/3	Body of corpus callosum
							Anterior corona radiate
	3						Left superior corona radiate
CAD *vs.* MMD	1	312	−26	−26	67	< 0.05/3	Anterior corona radiate
							Posterior thalamic radiation
	2	214	24	16	48	< 0.05/3	Superior longitudinal fasciculus

Results are bilateral unless a hemisphere is specified. *x*, *y*, *z*: Peak coordinates in MNI space. MNI: Montreal Neurological Institute; MMD: moyamoya disease; CAD: cerebrovascular atherosclerotic disease; NC: normal control.

damage to the frontal cortex caused by hemodynamic disturbances is a major cause of vascular cognitive impairment (Calviere et al., 2012; Lei et al., 2014; Chen et al., 2016; Fang et al., 2016). Additionally, the middle cingulate cortex is reported to be the main hub for the impulse control network. It connects to the frontal regions related to decision making and affects vascular cognitive impairment (Shackman et al., 2011). In the present study, gray matter atrophy was significant in the bilateral middle cingulate cortex and parts of the frontal gyrus in both moyamoya disease and cerebrovascular atherosclerotic disease groups, implying that vascular cognitive impairment might result from regional gray matter atrophy.

While gray matter comprises neuronal cell bodies, white matter is made from the myelinated axons that connect neurons to each other. In this study, white matter tract abnormalities were identified in the genu and body of corpus callosum, the anterior and superior corona radiations, and the posterior thalamic radiation in both moyamoya disease and cerebrovascular atherosclerotic disease, indicating that this pattern of damage to white matter tracts might be characteritic of vascular cognitive impairment. The corpus callosum is the largest white matter tract in the brain and plays a vital role in executive function, such as processing speed and problem solving abilities (van Eimeren et al., 2008; Penke et al., 2010). In addition, both the corona radiation and posterior thalamic radiation contain fibers that transfer information between the thalamus and the cerebral cortex. Their common pattern of white matter tract damage may be due to a common hemody-

namic disturbance (Schubert et al., 2014).

In the present study, the moyamoya disease group presented a widespread pattern of damage to gray and white matter, while the cerebrovascular atherosclerotic disease group presented a more central and medial pattern of damage. This implies a potential link between gray matter and white matter damage. There are two possible explanations. First, neuronal cell bodies and axons are parts of the same cell, and physiological and anatomical studies show that they often are impaired together under pathological conditions. For example, when white matter tracts deteriorate after demyelination, the signal conduction along the nerve is impaired, which leads to withering of the nerve and somatic atrophy. Kazumata et al. (2015) also noted a positive link between focally damaged gray and white matter in another MDD study. Subsequently, chronic hemodynamic deficiencies, inflammation, and other factors lead to unique collateral and microstructural damage in MDD and cerebrovascular atherosclerotic disease (Masuda et al., 1993; Vermeer et al., 2003; Bos et al., 2012; Blecharz et al., 2017). Furthermore, Schubert et al. (2014) also noticed territory-specific patterns of cerebral blood flow in a previous study comparing the two diseases. Thus, we speculated that vascular cognitive impairment is a heterogeneous complication and a consequence of both hemodynamic compromise and other coexisting disruptive factors.

In addition to describing the cognitive impairment of moyamoya disease and cerebrovascular atherosclerotic disease, this study is particularly interested in establishing a

methodology for detecting and monitoring disease progression in future studies of this particular patient population. Moreover, the data presented in this study can be used as a good cornerstone for monitoring the efficacy of surgical revascularization (Amin-Hanjani and Charbel, 2006).

Some limitations of this study should be considered. Primarily, the present study excluded patients with obvious structural abnormalities or early stage vascular cognitive impairment (Reis et al., 2013; Kazumata et al., 2015). Moreover, the small sample size limits the statistical power. Finally, tract-based spatial statistics and VBM analysis can only do group comparisons, but cannot do individual analysis. Additionally, it is technically difficult to balance type-I and type-II errors in terms of what corrective methods are used in the VBM analysis.

Taken together, the present study provides valuable information about the spatial patterns of microstructural damage in vascular cognitive impairment by comparing two chronic cerebrovascular diseases. Future studies are needed to explore the relationship between microstructural damage and cognitive performance in vascular cognitive impairment patients.

Institutional review board statement: *The study was approved by the Institutional Review Board in Huashan Hospital, China (approval No. 2014-278). All procedures performed in studies involving human participants were in accordance with the ethical standards of the institutional and/or national research committee and with the 1964 Helsinki declaration and its later amendments or comparable ethical standards.*
Declaration of participant consent: *The authors certify that they have obtained consent forms from the participants or their legal guardians. In the forms, the participants or their legal guardians have given consent for the participant images and other clinical information to be reported in the journal. The participants or their legal guardians understand that the participants' names and initials will not be published and due efforts will be made to conceal their identity.*
Reporting statement: *This study followed the STrengthening the Reporting of OBservational studies in Epidemiology (STROBE) guidance.*
Biostatistics statement: *The statistical methods of this study were reviewed by the biostatistician of Huashan Hospital of Fudan University in China.*
Copyright license agreement: *The Copyright License Agreement has been signed by all authors before publication.*
Data sharing statement: *Individual participant data that underlie the results reported in this article after deidentification (text, tables, figures, and appendices) will be shared. Study protocol, informed consent form and clinical study report will be promulgated within 6 months after the completion of the trial. Anonymized trial data will be available indefinitely at www.figshare.com.*
Plagiarism check: *Checked twice by iThenticate.*
Peer review: *Externally peer reviewed.*
Open peer reviewer: *Rodolfo Gabriel Gatto, University of Illinois at Chicago, USA.*
Additional files:
Additional file 1: Ethical review approval (Chinese).
Additional file 2: STROBE checklist.
Additional file 3: Open peer review report 1.

References

Amin-Hanjani S, Charbel FT (2006) Is extracranial-intracranial bypass surgery effective in certain patients? Neurol Clin 24:729-743.

Avelar white matter, D'Abreu A, Coan AC, Lima FO, Guimaraes R, Yassuda CL, Oliveira GP, Guillaumon AT, Filho AA, Min LL, Cendes F (2015) Asymptomatic carotid stenosis is associated with gray and white matter damage. Int J Stroke 10:1197-1203.

Balucani C, Silvestrini M (2011) Carotid atherosclerotic disease and cognitive function: mechanisms identifying new therapeutic targets. Int J Stroke 6:368-369.

Blecharz KG, Frey D, Schenkel T, Prinz V, Bedini G, Krug SM, Czabanka M, Wagner J, Fromm M, Bersano A, Vajkoczy P (2017) Autocrine release of angiopoietin-2 mediates cerebrovascular disintegration in Moyamoya disease. J Cereb Blood Flow Metab 37:1527-1539.

Bos D, Vernooij MW, Elias-Smale SE, Verhaaren BF, Vrooman HA, Hofman A, Niessen WJ, Witteman JC, van der Lugt A, Ikram MA (2012) Atherosclerotic calcification relates to cognitive function and to brain changes on magnetic resonance imaging. Alzheimers Dement 8:S104-111.

Calviere L, Ssi Yan Kai G, Catalaa I, Marlats F, Bonneville F, Larrue V (2012) Executive dysfunction in adults with moyamoya disease is associated with increased diffusion in frontal white matter. J Neurol Neurosurg Psychiatry 83:591-593.

Cao X, Guo Q, Zhao Q, Jin L, Fu J, Hong Z (2010) The neuropsychological characteristics and regional cerebral blood flow of vascular cognitive impairment-no dementia. Int J Geriatr Psychiatry 25:1168-1176.

Chen Y, Wang C, Liang H, Chen H, Bi Y, Sun H, Shi Q, Deng Y, Li J, Wang Y, Zhang Y (2016) Resting-state functional magnetic resonance imaging in patients with leukoaraiosis-associated subcortical vascular cognitive impairment: a cross-sectional study. Neurol Res 38:510-517.

Chua XY, Choo Rwhite matter, Ha NHL, Cheong CY, Wee SL, Yap PLK (2018) Mapping modified Mini-Mental State Examination (MMSE) scores to dementia stages in a multi-ethnic Asian population. Int Psychogeriatr doi: 10.1017/S1041610218000704.

Fang L, Huang J, Zhang Q, Chan RC, Wang R, Wan W (2016) Different aspects of dysexecutive syndrome in patients with moyamoya disease and its clinical subtypes. J Neurosurg 125:299-307.

Gorelick PB, Scuteri A, Black SE, Decarli C, Greenberg SM, Iadecola C, Launer LJ, Laurent S, Lopez OL, Nyenhuis D, Petersen RC, Schneider JA, Tzourio C, Arnett DK, Bennett DA, Chui HC, Higashida RT, Lindquist R, Nilsson PM, Roman GC, et al. (2011) Vascular contributions to cognitive impairment and dementia: a statement for healthcare professionals from the american heart association/american stroke association. Stroke 42:2672-2713.

Hachinski V, Iadecola C, Petersen RC, Breteler MM, Nyenhuis DL, Black SE, Powers WJ, DeCarli C, Merino JG, Kalaria RN, Vinters HV, Holtzman DM, Rosenberg GA, Wallin A, Dichgans M, Marler JR, Leblanc GG (2006) National Institute of Neurological Disorders and Stroke-Canadian Stroke Network vascular cognitive impairment harmonization standards. Stroke 37:2220-2241.

He J, Huang Y, Du G, Wang ZQ, Xiang Y, Wang QS (2018) Cognitive impairment and hippocampal alpha-synuclein change in a rat model of chronic cerebral hypoperfusion. Zhongguo Zuzhi Gongcheng Yanjiu 22:3230-3236.

Hua K, Zhang J, Wakana S, Jiang H, Li X, Reich DS, Calabresi PA, Pekar JJ, van Zijl PC, Mori S (2008) Tract probability maps in stereotaxic spaces: analyses of white matter anatomy and tract-specific quantification. Neuroimage 39:336-347.

Karzmark P, Zeifert PD, Bell-Stephens TE, Steinberg GK, Dorfman LJ (2012) Neurocognitive impairment in adults with moyamoya disease without stroke. Neurosurgery 70:634-638.

Kazumata K, Tha KK, Narita H, Kusumi I, Shichinohe H, Ito M, Nakayama N, Houkin K (2015) Chronic ischemia alters brain microstructural integrity and cognitive performance in adult moyamoya disease. Stroke 46:354-360.

Lei Y, Li YJ, Guo QH, Liu XD, Liu Z, Ni W, Su JB, Yang H, Jiang HQ, Xu B, Gu YX, Mao Y (2017a) Postoperative executive function in adult moyamoya disease: a preliminary study of its functional anatomy and behavioral correlates. J Neurosurg 126:527-536.

Lei Y, Su J, Guo Q, Yang H, Gu Y, Mao Y (2016) Regional gray matter atrophy in vascular mild cognitive impairment. J Stroke Cerebrovasc Dis 25:95-101.

Lei Y, Su J, Jiang H, Guo Q, Ni W, Yang H, Gu Y, Mao Y (2017b) Aberrant regional homogeneity of resting-state executive control, default mode, and salience networks in adult patients with moyamoya disease. Brain Imaging Behav 11:176-184.

Lei Y, Li Y, Ni W, Jiang H, Yang Z, Guo Q, Gu Y, Mao Y (2014) Spontaneous brain activity in adult patients with moyamoya disease: a resting-state fMRI study. Brain Res 1546:27-33.

Lu L, Bigler ED (2002) Normative data on trail making test for neurologically normal, Chinese-speaking adults. Appl Neuropsychol 9:219-225.

Marshall RS, Festa JR, Cheung YK, Pavol MA, Derdeyn CP, Clarke WR, Videen TO, Grubb RL, Slane K, Powers WJ, Lazar RM (2014) Randomized Evaluation of Carotid Occlusion and Neurocognition (RECON) trial: main results. Neurology 82:744-751.

Masuda J, Ogata J, Yutani C (1993) Smooth muscle cell proliferation and localization of macrophages and T cells in the occlusive intracranial major arteries in moyamoya disease. Stroke 24:1960-1967.

Meng D, Hosseini AA, Simpson RJ, Shaikh Q, Tench CR, Dineen RA, Auer DP (2017) Lesion topography and microscopic white matter tract damage contribute to cognitive impairment in symptomatic carotid artery disease. Radiology 282:502-515.

O'Brien JT, Erkinjuntti T, Reisberg B, Roman G, Sawada T, Pantoni L, Bowler JV, Ballard C, DeCarli C, Gorelick PB, Rockwood K, Burns A, Gauthier S, DeKosky ST (2003) Vascular cognitive impairment. Lancet Neurol 2:89-98.

Obara K, Fukuuchi Y, Kobari M, Watanabe S, Dembo T (1997) Cerebral hemodynamics in patients with moyamoya disease and in patients with atherosclerotic occlusion of the major cerebral arterial trunks. Clin Neurol Neurosurg 99 Suppl 2:S86-89.

Pantoni L, Garcia JH, Gutierrez JA (1996) Cerebral white matter is highly vulnerable to ischemia. Stroke 27:1641-1647.

Penke L, Munoz Maniega S, Murray C, Gow AJ, Hernandez MC, Clayden JD, Starr JM, Wardlaw JM, Bastin ME, Deary IJ (2010) A general factor of brain white matter integrity predicts information processing speed in healthy older people. J Neurosci 30:7569-7574.

Reis JP, Launer LJ, Terry JG, Loria CM, Zeki Al Hazzouri A, Sidney S, Yaffe K, Jacobs DR, Jr., Whitlow CT, Zhu N, Carr JJ (2013) Subclinical atherosclerotic calcification and cognitive functioning in middle-aged adults: the CARDIA study. Atherosclerosis 231:72-77.

Research Committee on the Pathology and Treatment of Spontaneous Occlusion of the Circle of Willis, Health Labour Sciences Research Grant for Research on Measures for Infractable Diseases (2012) Guidelines for diagnosis and treatment of moyamoya disease (spontaneous occlusion of the circle of Willis). Neurol Med Chir (Tokyo) 52:245-266.

Schubert GA, Czabanka M, Seiz M, Horn P, Vajkoczy P, Thome C (2014) Perfusion characteristics of Moyamoya disease: an anatomically and clinically oriented analysis and comparison. Stroke 45:101-106.

Shackman AJ, Salomons TV, Slagter HA, Fox AS, Winter JJ, Davidson RJ (2011) The integration of negative affect, pain and cognitive control in the cingulate cortex. Nat Rev Neurosci 12:154-167.

Smith SM (2002) Fast robust automated brain extraction. Hum Brain Mapp 17:143-155.

Soriano SG, Cowan DB, Proctor MR, Scott RM (2002) Levels of soluble adhesion molecules are elevated in the cerebrospinal fluid of children with moyamoya syndrome. Neurosurgery 50:544-549.

van Eimeren L, Niogi SN, McCandliss BD, Holloway ID, Ansari D (2008) White matter microstructures underlying mathematical abilities in children. Neuroreport 19:1117-1121.

van Oijen M, de Jong FJ, Witteman JC, Hofman A, Koudstaal PJ, Breteler MM (2007) Atherosclerosis and risk for dementia. Ann Neurol 61:403-410.

Vermeer SE, Prins ND, den Heijer T, Hofman A, Koudstaal PJ, Breteler MM (2003) Silent brain infarcts and the risk of dementia and cognitive decline. N Engl J Med 348:1215-1222.

Wakana S, Caprihan A, Panzenboeck MM, Fallon JH, Perry M, Gollub RL, Hua K, Zhang J, Jiang H, Dubey P, Blitz A, van Zijl P, Mori S (2007) Reproducibility of quantitative tractography methods applied to cerebral white matter. Neuroimage 36:630-644.

Wei M, Shi J, Li T, Ni J, Zhang X, Li Y, Kang S, Ma F, Xie H, Qin B, Fan D, Zhang L, Wang Y, Tian J (2018) Diagnostic accuracy of the Chinese version of the trail-making test for screening cognitive impairment. J Am Geriatr Soc 66:92-99.

Weinberg DG, Rahme RJ, Aoun SG, Batjer HH, Bendok BR (2011) Moyamoya disease: functional and neurocognitive outcomes in the pediatric and adult populations. Neurosurg Focus 30:E21.

Weinstein JD (2018) A new direction for Alzheimer's research. Neural Regen Res 13:190-193.

Wendell CR, Waldstein SR, Ferrucci L, O'Brien RJ, Strait JB, Zonderman AB (2012) Carotid atherosclerosis and prospective risk of dementia. Stroke 43:3319-3324.

Zhao H, Li Z, Wang Y, Zhang Q (2012a) Hippocampal expression of synaptic structural proteins and phosphorylated cAMP response element-binding protein in a rat model of vascular dementia induced by chronic cerebral hypoperfusion. Neural Regen Res 7:821-826.

Zhao Q, Lv Y, Zhou Y, Hong Z, Guo Q (2012b) Short-term delayed recall of auditory verbal learning test is equivalent to long-term delayed recall for identifying amnestic mild cognitive impairment. PLoS One 7:e51157.

STROBE Statement—Checklist of items that should be included in reports of *cross-sectional studies*

	Item No	Recommendation
Title and abstract	1	(*a*) Indicate the study's design with a commonly used term in the title or the abstract √
		(*b*) Provide in the abstract an informative and balanced summary of what was done and what was found √
Introduction		
Background/rationale	2	Explain the scientific background and rationale for the investigation being reported√
Objectives	3	State specific objectives, including any prespecified hypotheses √
Methods		
Study design	4	Present key elements of study design early in the paper √
Setting	5	Describe the setting, locations, and relevant dates, including periods of recruitment, exposure, follow-up, and data collection√
Participants	6	(*a*) Give the eligibility criteria, and the sources and methods of selection of participants√
Variables	7	Clearly define all outcomes, exposures, predictors, potential confounders, and effect modifiers. Give diagnostic criteria, if applicable√
Data sources/ measurement	8*	For each variable of interest, give sources of data and details of methods of assessment (measurement). Describe comparability of assessment methods if there is more than one group√
Bias	9	Describe any efforts to address potential sources of bias √
Study size	10	Explain how the study size was arrived at N/A
Quantitative variables	11	Explain how quantitative variables were handled in the analyses. If applicable, describe which groupings were chosen and why √
Statistical methods	12	(*a*) Describe all statistical methods, including those used to control for confounding √
		(*b*) Describe any methods used to examine subgroups and interactions NA
		(*c*) Explain how missing data were addressed N/A
		(*d*) If applicable, describe analytical methods taking account of sampling strategy√
		(*e*) Describe any sensitivity analyses NA
Results		
Participants	13*	(a) Report numbers of individuals at each stage of study—eg numbers potentially eligible, examined for eligibility, confirmed eligible, included in the study, completing follow-up, and analysed √
		(b) Give reasons for non-participation at each stage NA
		(c) Consider use of a flow diagram √
Descriptive data	14*	(a) Give characteristics of study participants (eg demographic, clinical, social) and information on exposures and potential confounders√
		(b) Indicate number of participants with missing data for each variable of interest N/A
Outcome data	15*	Report numbers of outcome events or summary measures√
Main results	16	(*a*) Give unadjusted estimates and, if applicable, confounder-adjusted estimates and their precision (eg, 95% confidence interval). Make clear which confounders were adjusted for and why they were included √
		(*b*) Report category boundaries when continuous variables were categorized NA
		(*c*) If relevant, consider translating estimates of relative risk into absolute risk for a

		meaningful time period NA
Other analyses	17	Report other analyses done—eg analyses of subgroups and interactions, and sensitivity analysesNA

Discussion

Key results	18	Summarise key results with reference to study objectives √
Limitations	19	Discuss limitations of the study, taking into account sources of potential bias or imprecision. Discuss both direction and magnitude of any potential bias √
Interpretation	20	Give a cautious overall interpretation of results considering objectives, limitations, multiplicity of analyses, results from similar studies, and other relevant evidence √
Generalisability	21	Discuss the generalisability (external validity) of the study results √

Other information

Funding	22	Give the source of funding and the role of the funders for the present study and, if applicable, for the original study on which the present article is based √

*Give information separately for exposed and unexposed groups.

Note: An Explanation and Elaboration article discusses each checklist item and gives methodological background and published examples of transparent reporting. The STROBE checklist is best used in conjunction with this article (freely available on the Web sites of PLoS Medicine at http://www.plosmedicine.org/, Annals of Internal Medicine at http://www.annals.org/, and Epidemiology at http://www.epidem.com/). Information on the STROBE Initiative is available at www.strobe-statement.org.